Electron paramagnetic resonance measurements near the tricritical point in $BaTiO_3$

D. L. Decker, Ke Huang,* and H. M. Nelson
Department of Physics and Astronomy, Brigham Young University, Provo, Utah 84602
(Received 28 March 2002; revised manuscript received 19 August 2002; published 8 November 2002)

We report electron paramagnetic resonance measurements on $BaTiO_3$, containing a dilute impurity of Fe^{3+}, in its ferroelectric phase over a range of pressure and temperature near the paraelectric-ferroelectric phase transition line. We have developed an algorithm to analyze the data, allowing us to determine the values of the crystal field parameters and their temperature and pressure dependence required to reproduce the measured spectra. Then, using the Landau free energy expansion to sixth order in the order parameter and noting that the tetragonal distortion field D is proportional to the square of the order parameter, we determine the Landau parameters and get a value for the tricritical point for $BaTiO_3$.

DOI: 10.1103/PhysRevB.66.174103 PACS number(s): 61.50.Ks, 64.60.Kw, 64.70.Kb

I. INTRODUCTION

The series of phase changes in the ABO_3 family of perovskites ranks among the most extensively studied of all structural phase transitions. $BaTiO_3$, a member of this family, is a prototype ferroelectric and has widespread applications in nonlinear optics and electro-optics. Its transition from the cubic-paraelectric state to the tetragonal-ferroelectric state results from a tetragonal distortion below the transition temperature T_c. As discussed by Samara,[1] this first-order, cubic-to-tetragonal, transition in $BaTiO_3$ changes to second order above a certain pressure. The point on the phase line where the order of the transition changes is called a tricritical point.[2] This transition, originally believed to be purely displacive, may have some order-disorder characteristics also.[3]

A displacive phase transition involves a shift of some atoms by small amounts from their symmetry positions in the higher-symmetry phase. The new positions change the symmetry and thus create a new crystal structure. Order-disorder transitions involve a disordered state, in the high-symmetry phase, in which the atoms are dynamically distributed uniformly over a set of equivalent sites which average to a symmetry position in the higher-symmetry phase, and at the transition the distribution changes to favor a subset of the equivalent sites which results in a new crystal symmetry.[4]

One can associate an order parameter with a change in an ion's position relative to the unit cell for a displacive transition or the occupation of the various equivalent sites for an order-disorder transition. In the ferroelectric phase of $BaTiO_3$ the Ti^{4+} ion and its cage of O^{2-} ions are displaced relative to each other such as to create an electric dipole moment in each unit cell. This displacement can be used as the order parameter of the transition. Thus the order parameter is zero in the cubic phase, but in the ferroelectric phase the electric polarization vector, which is proportional to this displacement, can be used as the order parameter. A phase transition is considered first order if the order parameter changes discontinuously at the transition.

It appears to be a general property of second-order structural phase transitions to involve a lowering in the frequency of some vibrational mode, a ''softening,'' as T_c is approached. As the mode frequency decreases, the amplitude of vibration becomes larger and the anharmonic terms in the interatomic potential become more important near T_c. The structure of the new phase is determined by the eigenvector of the soft mode and the parent phase. The eigenvector of the mode is the array of atomic displacements relative to the lattice sites and is equivalent to the order parameter of the transition.

In a pressure- (P-) temperature (T) thermodynamic phase diagram, a critical point marks the end of a line of coexistence where two distinct coexisting phases become identical. If one considers a system with three thermodynamic variables, i.e., an electric field **E** in addition to P and T, then a critical point in P-T plane will become a continuous line of critical points in the P-T **E** space. These are lines of continuous phase transitions. Landau argued that a second-order continuous coexistence line separating two phases of different symmetry cannot end in a point and proposed that such a line would have to terminate by changing into a first-order transition line. This point is called a tricritical point.[5] When viewed in a space of suitable thermodynamic variables, a tricritical point may be defined as the end point of a line of triple points at which three coexisting phases simultaneously become identical. Indeed, the term ''tricritical point'' was originally introduced by Griffith to indicate the confluence of three lines of ordinary critical points.[2]

At atmospheric pressure T_c is about 136 °C for pure barium titanate but is lowered by impurities such as iron in the lattice. Below T_c, at room temperature, the c axis is elongated about 0.6% and the a axes are shortened by about 0.3%, changing the symmetry from cubic to tetragonal. The tetragonal distortion alone does not produce the electric polarization but rather the rearrangement of the ions within the new unit cell. The Ti^{4+} ion, which was in the center of an oxygen cage, is displaced along the new c axis in a direction opposite to the displacement of the oxygen cage, thus creating a permanent electric dipole moment.[6] There is strong evidence that the transition is associated with the instability of one of the optical phonon modes of the lattice. As the frequency of the relevant mode decreases and finally becomes unstable at the transition, the crystal transforms to the tetragonal phase. Whether the transition is purely displacive or partly order-disorder has not been answered definitively.

Several researchers have made measurements that have

hinted at a tricritical point in $BaTiO_3$. This was first suggested by Polandov *et al.*[7] who measured the effects of pressure to 10 kbar on the magnitude of the jump in the spontaneous polarization (P_s) at the ferroelectric transition. He discovered ΔP_s^2 to decrease linearly with pressure and extrapolated it to go to zero at 17 kbar. This was the first estimate of the tricritical point. Samara[1] presented dielectric constant measurements to 19 kbar and noted that the transition still showed definite first-order behavior but a continuing trend toward becoming second order. From this he predicted the tricritical point to be in the range of 30–40 kbar. Clark and Benguigui[8] reported experimental measurements of a pressure-induced tricritical point at 34 kbar and 18 °C. Their results were probably affected by the sensitivity of this transition to nonhydrostatic stress. Decker and Zhao[9] made dielectric and polarization measurements in a hydrostatic medium to 38 kbar and reported that the phase transition appeared to go from first to second order near 35 kbar and −40 °C. They looked at both pure $BaTiO_3$ and butterfly crystals which have different phase lines and tricritical points because of their impurity content.

The object of this work was to use a more sensitive probe to observe the symmetry changes in the $BaTiO_3$ crystal structure. For this purpose we employed electron paramagnetic resonance (EPR), which is a good technique to study phase transitions because of its sensitivity to local symmetry changes in the crystal. This required the development of an apparatus which could make precision EPR measurements on single crystals in a hydrostatic environment over a region of pressures and temperatures never before accomplished. This study will contribute to a better understanding of the tetragonal-cubic phase transition and the tricritical point in $BaTiO_3$.

EPR is carried out by introducing into the lattice a paramagnetic probe ion in low concentration. Transition-metal ions such as Fe^{3+} having a half-filled *d* shell are particularly useful as probe ions. EPR studies of crystal symmetries and structural phase transitions have been pioneered by Müller and others in his laboratory.[10,11] Hornig *et al.*[12] made the first study of barium titanate. Since the ionic radius of Fe^{3+} is 0.64 Å, which is close to that of the Ti^{4+}, 0.68 Å, it was assumed that Fe^{3+} substitutes for Ti^{4+} on the octahedral site. This assumption has been verified by Siegel and Müller[13] using Newmann superposition theory.

We introduce here the spin Hamiltonian **H**, in tetragonal symmetry, to facilitate further discussion of EPR results:

$$\mathbf{H}=\beta\mathbf{B}\cdot\vec{g}\cdot\mathbf{S}+DS_z^2+aS_z^4+b(S_x^4+S_y^4), \qquad (1)$$

where β is the Bohr magneton, **B** is the magnetic field vector, and **S** is the spin operator with components S_x, S_y, S_z. The gyromagnetic ratio $\vec{g}$, is a 3×3 diagonal tensor which has two independent elements $g_\parallel$ and $g_\perp$ for the directions parallel and perpendicular to the *c* axis. *D*, *a*, and *b* are crystal-field parameters. Because of the half filled *d* shell in Fe^{3+} the orbital angular momentum is quenched and this becomes an exact Hamiltonian.[14]

Rimai and deMars[15] showed that *D*, measured with both Gd^{3+} and Fe^{3+} probes in $BaTiO_3$, was proportional to the lattice distortion and the square of the electric polarization in the ferroelectric phase. Sakudo[16] studied the change of the crystal-field parameters of $BaTiO_3$ at the phase transition and also the effect of a dc electric field on the phase transitions in $BaTiO_3$. Müller and Berlinger[17] measured the pressure dependence of the cubic-crystalline field-splitting parameter *a* to 3 kbar. [Note their *a* is 6 times larger than that defined in Eq. (1).] They argued that the tetragonal-cubic transition in $BaTiO_3$ is more order-disorder in nature than displacive.

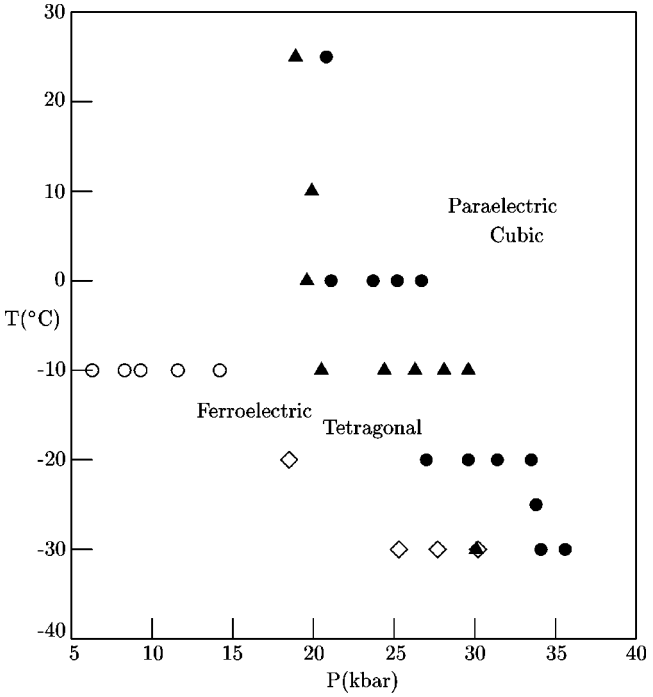

FIG. 1. The positions in pressure-temperature space where sets of data were taken. The different symbols show the data sets from different runs. All measurements shown were in the tetragonal phase.

Several years ago Ellwanger[18] made the first EPR measurements in a pressure apparatus on $BaTiO_3$ butterfly crystals. The resonance peaks were very broad and the results had large uncertainties. Part of this work was published.[19] Our measurements are the first precision high-pressure EPR studies on a good single crystal of this material.

II. EXPERIMENTAL MEASUREMENT

A detailed description of the apparatus is given in the dissertation by Huang[20] and has already been published.[21] Briefly, we directed *X*-band radiation from a klystron into a right-circular-cylinder single-crystal sapphire of dimensions such as to be resonant in the TM_{110} mode at ~9.3 GHz. The sapphire also served as one anvil of a high-pressure press. The other anvil was of titanium carbide. Between the two anvils was an Inconel 718 gasket of 0.3 mm thickness containing a hole of 1.1 mm diameter into which the sample and a small ruby fragment were placed. This hole was filled with petroleum ether to serve as a hydrostatic pressure medium. The sapphire was enclosed in a thin-walled copper can with openings to provide for coupling the microwaves to the cav-

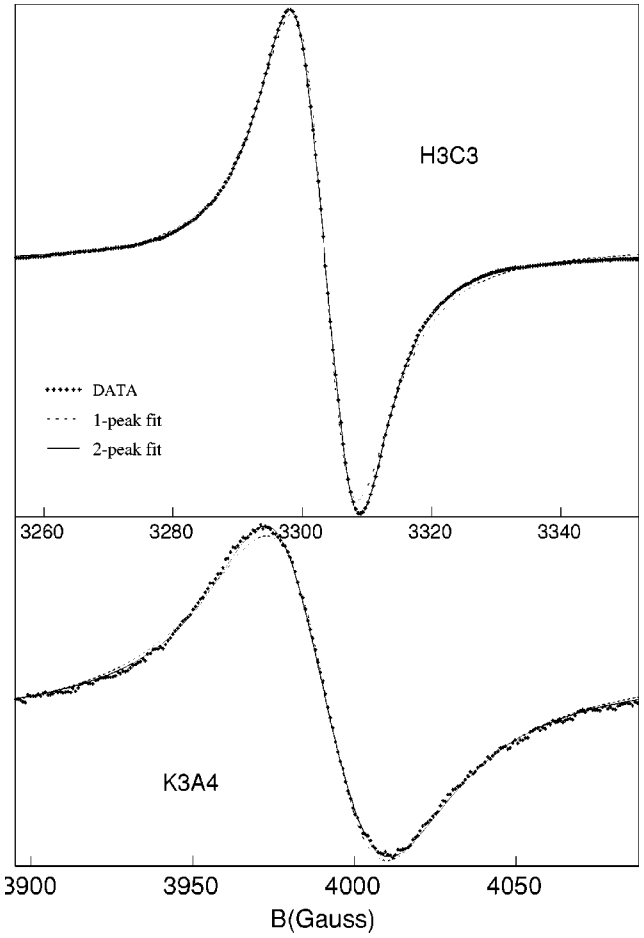

FIG. 2. Resonance signals of $c3$ and $a4$ spectral lines vs magnetic field. Also shown is the least-squares fitting using a single Lorentzian derivative line shape and two slightly separated Lorentzian derivative spectra.

ity and optical access for directing an argon laser beam onto the ruby to measure the pressure in the cell.[22]

Modulation coils modulated the magnetic field at 100 kHz, and the dc magnetic field supplied by an electromagnet was calibrated at the sample position with an NMR probe. The estimated field reproducibility was about ± 0.4 G. The EPR spectrometer recorded the derivative signal on a data file which could then be analyzed by computer.

We employed a small single-crystal of $BaTiO_3$ doped with 0.03 at. % Fe_2O_3 which was grown by J. Albers using the top-seeded solution technique.[23] After orienting the crystal we used a wire saw to cut off a thin plate such that an *a* axis was normal to the plate and thus the plane of the plate contained the *c* axis and the other *a* axis. It was polished to a final thickness of 0.1 mm, and circular disks of 0.9 mm diameter were cut from the plate using a rotating ''cookie'' cutter and 600-grit SiC abrasive. The disk when placed in the high-pressure cell was easily oriented such that the magnetic field could be pointed parallel to the *a* or *c* axis merely by rotating the magnet through 90°. The pressure cell was attached to the cold head of a Displex helium gas refrigerator, and the system was surrounded by a vacuum chamber contained between the pole faces of the magnet. In this manner

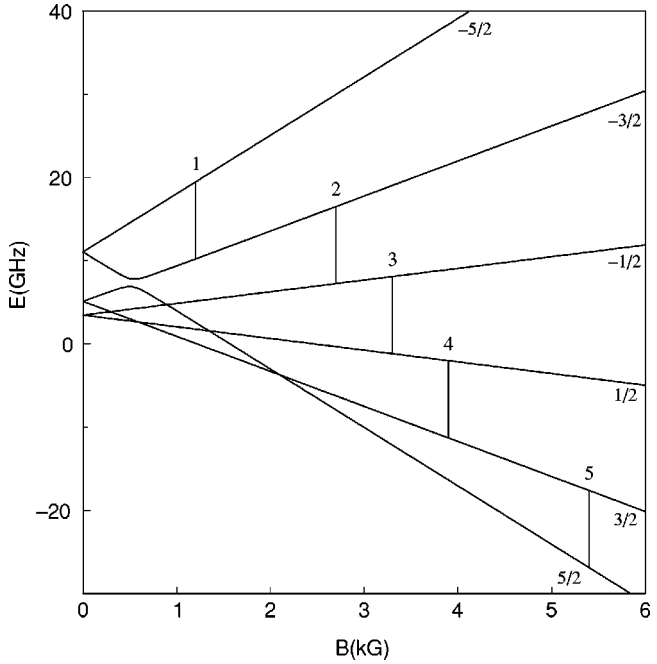

FIG. 3. Magnetic-field dependence of the eigenenergies of spin 5/2 with the crystal *c* axis oriented along the magnetic field. The eigenenergies are labeled with the dominant spin component. The EPR resonances observed at a klystron frequency of 9.28 GHz are shown along with the way we labeled them.

it was possible to cool the entire cell to temperatures of the order of 40 K. We controlled the temperature by an Air Product temperature controller and a heating element attached to the cooling head of the refrigerator. Temperatures could be controlled and measured to an accuracy of ± 0.3 K.

We made EPR measurements at several pressures and temperatures in the ferroelectric phase near the phase transition; see Fig. 1. We tried to stay below the tetragonal-cubic transition because after passing the crystal into the cubic phase it would usually return to the tetragonal phase in a multidomain state, especially as one approaches the tricritical point where there is very little difference between the domains. The points shown in Fig. 1 came from four different runs, each terminating after once crossing the phase line or when the sample was crushed by the deformation of the gasket under high pressure. Our measurements below $-30\,^{\circ}$C were also unusable because the surrounding fluid became nonhydrostatic and the strains would create multidomains in the sample. The results from the 30 sets of data, each set containing 1–5 resonances with the magnetic field along the *c* axis and 1–5 resonances with the field along the *a* axis, were collected on a computer and then analyzed as described in the following section. These data are noted in the figure, and the different symbols designate to which run each data point belonged.

III. ANALYSIS

The EPR spectral lines are derivatives of a Lorentzian-shaped signal, and ideally they should be represented by the expression below where $R(B)$ is the resonance signal as a

function of the magnetic field B:

$$R(B) = -Y_{pp}B_{pp}^3(B-B_r) \Big/ \left((B-B_r)^2+\frac{3}{4}B_{pp}^2\right)^2, \quad (2)$$

where Y_{pp} and B_{pp} are the peak-to-peak signal height and peak-to-peak field width and B_r is the center-field position of the resonance.

The measured resonance shapes are slightly unsymmetric and a nonlinear least-squares fitting of them to Eq. (2) revealed that each was a combination of two strongly overlapped Lorentzian derivatives. Fitting the resonance to two overlapped peaks each with the shape in Eq. (2) gave a χ^2 value some 3–6 times smaller than for a single such line. In all of these double resonances one of the peaks had 3 ± 0.5 times the integrated intensity of the other. We chose the position of the resonance line as the weighted average position of the two individual resonances. Figure 2 shows two resonance spectra and the computer fit to the data. The superiority of the two-peak fit as compared to a one-peak fit is easily observed in the figure.

We are not as yet prepared to discuss the cause of the peak doubling. It may be due to the presence of vacancies causing different environments surrounding the Fe^{3+} EPR probes or if the transition is order-disorder the Fe^{3+} ions may not be in sites of exact tetragonal symmetry.

We labeled the various resonances as B_{ai} and B_{ci} where the subscripts a and c mean the data was taken with the field **B** along the a or c axis, respectively, and i goes from 1 to 5 for the five principal transitions between the respective energy levels. We refer to the transitions between the spin eigenstates labeled by their dominant z component of spin—i.e., $-\frac{3}{2}$ to $-\frac{5}{2}$, $-\frac{1}{2}$ to $-\frac{3}{2}$, $\frac{1}{2}$ to $-\frac{1}{2}$, $\frac{3}{2}$ to $\frac{1}{2}$, and $\frac{5}{2}$ to $\frac{3}{2}$, respectively, as shown in Fig. 3. The transitions resulted when the energy difference between the eigenvalues equaled the klystron frequency, and these are shown by the vertical lines in the figure. We labeled the different resonances 1–5 as shown in the figure.

The spin Hamiltonian of Eq. (1) can be written in matrix form using the standard representation of the spin-5/2 subspace as the basis vectors:

$$\mathbf{H}=\begin{pmatrix}
\frac{5}{2}p+\xi & \sqrt{5}q & 0 & 0 & \sqrt{45}b & 0 \\
\sqrt{5}q^* & \frac{3}{2}p+\eta & \sqrt{8}q & 0 & 0 & \sqrt{45}b \\
0 & \sqrt{8}q^* & \frac{1}{2}p+\zeta & 3q & 0 & 0 \\
0 & 0 & 3q^* & \zeta-\frac{1}{2}p & \sqrt{8}q & 0 \\
\sqrt{45}b & 0 & 0 & \sqrt{8}q^* & \eta-\frac{3}{2}p & \sqrt{5}q \\
0 & \sqrt{45}b & 0 & 0 & \sqrt{5}q^* & \xi-\frac{5}{2}p
\end{pmatrix}, \quad (3)$$

where

$$p=g_{\|}\beta B, \quad q=0, \qquad \text{for} \quad B\|c \ \text{ axis},$$

$$p=0, \quad q=\frac{1}{2}g_{\perp}\beta B, \qquad \text{for} \quad B\|a \ \text{ axis},$$

$$\xi=25D/4+625a/16+65b/8, \quad (4)$$

$$\eta=9D/4+81a/16+241b/8,$$

$$\zeta=D/4+a/16+401b/8.$$

There will be six eigenvalues corresponding to the six spin states m of the spin-5/2 manifold. The principal resonances result from the five dominant transitions between these eigenstates with $\Delta m=\pm1$. The gyromagnetic ratio $g_{\|}$ can be calculated directly from the $\frac{1}{2}$ to $-\frac{1}{2}$ transition measured with **B** parallel to the c axis. The other parameters must be deduced from the spectra with **B** aligned along the a and c axes.

A. First approach to extracting the crystal-field parameters

With the field along the c axis, where $q=0$, the spin Hamiltonian can be diagonalized algebraically using MAPLE V to get the eigenenergies E_i. The subscript i orders them by ascending energy at a large magnetic field, as a function of $g_{\|}, B, D, a$, and b. Then we solve Eq. (5) shown below, for the resonance field, B_{ci} where h is Planck's constant and ν_i is the klystron frequency at the ith resonance line:

$$E_{i+1}-E_i=h\nu_i. \quad (5)$$

This gives us the field positions of the five principal resonances with the field along the c axis. This equation for $i=3$ can be solved for $g_{\parallel}$, i.e.,

$$g_{\parallel}=h\nu_3/\beta B_{c3}. \tag{6}$$

The other equations for $i=1$, 2, 4, and 5 give fourth-order equations and are not readily solvable. We therefore substituted, into Eq. (5), $B_{ci}=B_{mi}+h_{ci}$, $D=D_0+d$, $a=a_0+\delta a$, and $b=b_0+\delta b$, where B_{mi} is the measured value of the field at the resonance, and D_0, a_0, and b_0 are estimates for these crystal-field parameters for that particular data set. We then expanded Eq. (5) to lowest order in h_{ci}, d, δa, and δb with $g_{\parallel}$ taken from Eq. (6) and ν_i being the measured resonance frequency. Solving we get h_{ci} as a function of $(d,\ \delta a,\ \delta b)$.

For the spectrum taken with the field along the a axis one must take a different approach since the Hamiltonian matrix cannot be diagonalized analytically. We first block diagonalize the matrix into two 3×3 blocks using the unitary transformation which has $+\sqrt{\frac{1}{2}}$ along the three top elements of the principal diagonal and all along the secondary diagonal and $-\sqrt{\frac{1}{2}}$ for the lower three elements of the principal diagonal to get

$$\mathbf{H}=\begin{pmatrix} \xi & \sqrt{5}(q+3b) & 0 & 0 & 0 & 0 \\ \sqrt{5}(q+3b) & \eta & \sqrt{8}q & 0 & 0 & 0 \\ 0 & \sqrt{8}q & \zeta+3q & 0 & 0 & 0 \\ 0 & 0 & 0 & \zeta-3q & \sqrt{8}q & 0 \\ 0 & 0 & 0 & \sqrt{8}q & \eta & \sqrt{5}(q-3b) \\ 0 & 0 & 0 & 0 & \sqrt{5}(q-3b) & \xi \end{pmatrix}, \tag{7}$$

with q,ξ,η, and ζ defined as functions of B,D,a,b, and $g_{\perp}$ by Eq. (4).

One then chooses initial values for $D=D_0$, $a=a_0$, $b=b_0$, $g_{\perp}=g_{\parallel}=g_0$, where $g_{\parallel}$ is taken from the analysis along the c axis; and $B_{ai}=B_{mi}$, the measured values of the resonance fields. This turns Eq. (7) into a numerical matrix $\mathbf{H}_0$. $\mathbf{H}_0$ is then diagonalized using the Jacobi method for each of its two blocks. Then we make the substitution $D=D_0+d$, $a=a_0+\delta a$, $b=b_0+\delta b$, $g_{\perp}=g_0+\gamma$, and $B_{ai}=B_{mi}+h_{ai}$, into the Hamiltonian matrix, Eq. (7), and proceed using the same transformation matrices that diagonalized $\mathbf{H}_0$. We conclude with a second-order perturbation calculation to get the final eigenenergies. Putting these eigenenergies into Eq. (5) and expanding to lowest order in the parameters d, $\delta a,\delta b,\gamma$, and h_{ai}, we solve for the five principal transition fields $h_{ai}(d,\delta a,\delta b,\gamma)$.

Since h_{ci} and h_{ai} are the differences between the calculated and measured resonance fields, we minimize $\Sigma[(h_{ci}/\delta B_c i)^2+(h_{ai}/\delta B_{ai})^2]$ by varying d, δa, δb, and γ, where δB_{ci} and δB_{ai} are the uncertainties in the measured resonance fields determined in the least-squares fitting to the line positions. This gives us a new set of values D_0,a_0,b_0, and g_0 to start the iteration over again until convergence is attained.

In this manner we could determine a value of the crystal field parameters for 28 of the 30 sets of data which had greater than 5 measured resonances. These results are given in Huang's dissertation.[20] However, 3 of these sets had only 6 measured resonances and thus only 1 degree of freedom, and 9 had only 2 degrees of freedom, so there was considerable scatter or uncertainty in the results. It was also noted that plotting a and $g_{\parallel}$ versus D along isotherms showed systematic variations with temperature. Thus we decided upon a more sophisticated analysis to allow us to use all the data and remove most of the scatter.

B. More sophisticated analysis of the data

At this point we consider the following. The parameter D varies as the square of the order parameter[15] jumping from zero in the cubic phase to a finite value in the tetragonal phase where the transition is first order or rising with an initial infinite slope upon entering the tetragonal phase where the transition is second order. In the cubic phase the crystal field parameters $a=b$, but they separate discontinuously or with an initial infinite slope upon entering the tetragonal phase, depending on the order of the transition. The same is true for $g_{\parallel}$ and $g_{\perp}$. Thus we assume that $g_{\perp}-g_{\parallel}$ and $b-a$ are both proportional to D with the average value of $(a+2b)/3$ and $(g_{\parallel}+2g_{\perp})/3$ being simple functions of pressure and temperature. According to the experimental results of Müller and Berlinger[17] they may be taken as linear functions. We let

$$\begin{aligned} a_k&=a_0+pP_k+tT_k-2nD_k, \\ b_k&=a_k+3nD_k \\ g_{\parallel k}&=g_0+\rho P_k+\tau T_k-2fD_k, \\ g_{\perp k}&=g_{\parallel_k}+3fD_k. \end{aligned} \tag{8}$$

a_0 and g_0 are the values of $\langle a\rangle$ and $\langle g\rangle$ at some chosen point in the P, T plane. We choose this point to be the tricritical

point (P_c, T_c). To start the fitting, we initially make an intelligent guess for P_c and T_c. The k's index each data set where P_k and T_k are its pressure and temperature relative to the tricritical point. We then did a least-squares fit to the entire set of the 220 resonance lines simultaneously with the 38 variable parameters a_0, p, t, n, g_0, ρ, τ, f, and D_k for each k from 1 to 30. This left 182 degrees of freedom.

This analysis was done by creating another MAPLE V program in a manner similar to the algorithm explained above. Beginning with an initial set of values for the D_k's and for $a_0, p, t, n, g_0, \rho, \tau$, and f, we again did the least-squares fitting of the spin Hamiltonians in both the a and c directions for all sets of resonance-field values. The least-squares fitting program also determined a statistical error for each of the variable parameters. There was one other correction that was made to the data. The resonances along the a-axis measurement seemed always to disagree slightly from those along the c axis. We therefore assumed that the process of rotating the magnet may give an offset to the field measurement. All the field calibrations were taken with the magnet aligned along the direction where we positioned the c axis of the crystal. We therefore subtracted a small amount from the resonance field values for the a axis measurements and varied the amount subtracted to give a minimum in the χ^2 of the fit discussed above. This amounted to a 2.3 G correction.

IV. RESULTS

The results of the analysis are given in Table I. With the high precision of the measurement and the method of analysis the values of D, at each point, are accurate to ± 0.006 to ± 0.014 GHz (2σ), for all points except the point nearest the transition where $D = 0.067(26)$ GHz. From the results in the table one can calculate a and b, as well as $g_\parallel$ and $g_\perp$ at any pressure and temperature where D is known using Eqs. (8). For example at room temperature and zero pressure where $D \simeq 2.7$ GHz, we calculate $g_\parallel = 2.0070 \pm 0.0006$ and $g_\perp = 2.0096 \pm 0.0006$ which are in good agreement with Hornig *et al.*[12] who reported $g_\parallel = 2.00 \pm 0.01$.

We now turn to an analysis of the temperature and pressure dependence of D. Since D is proportional to the square of the order parameter, we begin with the Landau expansion of the free energy near the phase transition in the tetragonal phase:

$$G = G_0 + AP_s^2 + BP_s^4 + CP_s^6, \tag{9}$$

where G_0 is the Gibbs free energy of the cubic phase, and P_s is the polarization, which can be considered the order parameter. This is a mean-field analysis. The coefficient A must vary with temperature and pass through zero at the phase transition. In a like manner it must also be a function of pressure. Huibregste and Young[24] showed a significant temperature dependence of B and we would include pressure dependence. The parameter C must be everywhere positive for stability.

The minima of $G(P_s)$ define the physical states of the system. If the minimum is at $P_s = 0$, then the cubic phase is the stable state, but if the minimum is at $P_s \neq 0$, then the tetragonal-ferroelectric state is the stable state. There is a root of $G' \equiv dG/dP_s = 0$ at $P_s = 0$ and other roots found from $G'/P_s = 0$. Since G, G'/P_s, and G'' are all functions of P_s^2, we will define $Q = P_s^2$. We now calculate the value of Q at the minimum of G to get the result

$$Q = -\frac{B}{3C} + \sqrt{\left(\frac{B}{3C}\right)^2 - \frac{A}{3C}}. \tag{10}$$

As we mentioned above, D is proportional to the square of the order parameter; thus D is proportional to Q. In the neighborhood of the tricritical point we let A and B be linear functions of pressure and temperature and C be a constant, so from Eq. (10)

$$D = -\epsilon[T - T_c + s(P - P_c)] + \sqrt{\epsilon^2[T - T_c + s(P - P_c)]^2 - \alpha[T - T_c + r(P - P_c)]}, \tag{11}$$

where α, ϵ, r, and s are constants while T_c and P_c are the temperature and pressure at the tricritical point.

To justify the above arguments we refer to a paper by Íñiguez *et al.*[25] They made a first-principles study of $BaTiO_3$ and found that the sixth-order potential expansion properly accounts for the system over a large range of temperature, but the temperature dependence of the coefficients was not a trivial function. However, an examination of their figure showing the explicit temperature dependence of the coefficients from 0 to 350 K reveals that a linear dependence of A and B and a constant C is a very good approximation over the range of temperatures in this experiment.

The measured values for the tetragonal distortion D were fitted to Eq. (11) by least squares analysis with a C++ nonlinear least-squares program, with α, ϵ, T_c, P_c, s, and r as variable parameters to get the following results:

$$\alpha = 0.04002(46), \quad \epsilon = 0.00312(23),$$
$$T_c = -32.6(5.8)\,^\circ\text{C}, \quad P_c = 36.8(1.6)\ \text{kbar}, \tag{12}$$
$$r = 3.684(41)\ \text{K/kbar}, \quad s = 8.09(60)\ \text{K/kbar}.$$

These results of the fitting are shown in Fig. 4 where we compare the values of D measured along isotherms versus

TABLE I. The parameters, determined in the fitting, for calculating $g_\parallel$ and $g_\perp$ and a and b as shown in Eqs. (8). D in GHz and the tricritical point $P_c = 36.8$ kbar and $T_c = -32.6\,^\circ$C. Other values for $\partial\langle a\rangle/\partial P$ and $\partial\langle a\rangle/\partial T$ are also shown.

g_0	$\tau(\text{K}^{-1})$	$\rho(\text{kbar}^{-1})$	$f(\text{GHz}^{-1})$
2.00 627(15)	0.000 393(61)	0.000 126(11)	0.000 330(38)
a_0 (GHz)	t (GHz/K)	p (GHz/kbar)	n
0.068 28(15)[a]	0.000 0059(56)	0.000 523 9(87)	0.000 593(48)
	−0.000 020[b]	0.0013	
	−0.000 21[c]	−0.0010	

[a]This paper.
[b]Reference 17.
[c]Reference 19.

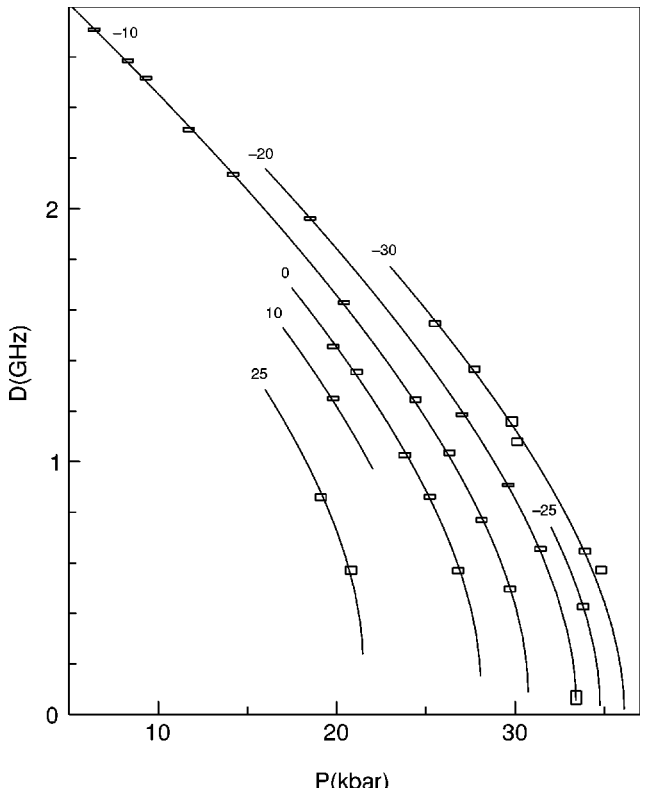

FIG. 4. The measured values of D vs P along the temperature isotherms and the least-squares fitted curves. The temperature of each curve is indicated in degrees Celsius.

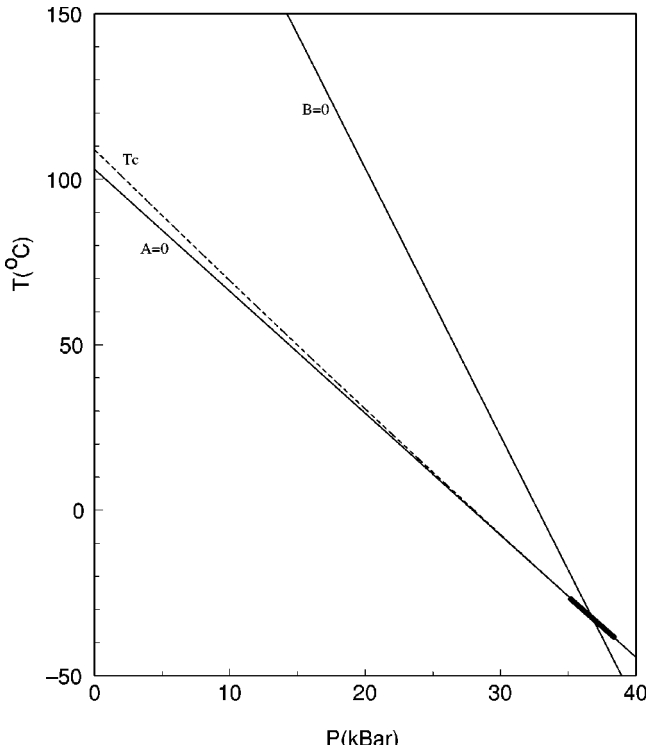

FIG. 5. The phase diagram of $BaTiO_3$ showing lines that separate regions of positive and negative Landau parameters A and B and the phase line between the tetragonal and cubic phases. The region of the tricritical point is also indicated by a solid bar.

the results calculated from Eq. (11) using the values of α, ϵ, T_c, P_c, r, and s shown above. We show in Fig. 5 the P, T phase plane of the region near the ferroelectric-paraelectric transition. Shown in this figure are the calculated lines where the Landau parameters $A=0$ and $B=0$, and the transition line where the Gibbs free energies of the cubic and tetragonal phases are equal. The point where both A and B are zero is the tricritical point. The transition extrapolates to $109 \pm (6)$ °C at atmospheric pressure which is reasonable for a sample with iron impurities. There is a strong correlation between T_c and P_c in the fitting so the minimum of χ^2 lies along a trough as shown in the figure.

V. CONCLUSIONS

We have presented a unique analysis of high-precision EPR data which allows a precise study of the pressure and temperature depence of the crystal-field parameters in $BaTiO_3$. The analyses of former EPR measurements on $BaTiO_3$ have approximated the spin Hamiltonian by assuming $D \gg a,b$, $a=b$, and $g_\perp = g_\parallel$. The only former results with narrow enough resonance lines to get precision measurements are those by Müller and Berlinger.[17] It is important to use single crystals with the smallest amount of strain possible to achieve sufficiently narrow resonance lines to determine the line positions accurately. We have shown that it is possible to determine individually a and b as well as $g_\parallel$ and $g_\perp$ using such a $BaTiO_3$ crystal, with careful calibration of the magnetic field and precision measurements of the klystron frequency. In this manner we were able to determine the crystal-field parameters by fitting the resonance measurements to the exact spin Hamiltonian without approximating the eigenvalues or ignoring differences between small terms. The average value of a and b is $\langle a \rangle = (a+2b)/3$ and of $g_\parallel$ and $g_\perp$ is $\langle g \rangle = (g_\parallel + 2g_\perp)/3$. Then by making a linear approximation for the temperature and pressure dependence of these average values along with the proposition that the differences $b-a$ and $g_\perp - g_\parallel$ are proportional to D; we are able to analyze all the data simultaneously. The assumption of $b-a$ being proportional to D seems reasonable since $b-a$ and D both depend upon symmetry breaking from the cubic phase. The dependence of $g_\perp - g_\parallel$ on D was also assumed to be linear, but the measured resonances could be fitted equally well if the dependence was quadratic.

The temperature and pressure dependence of $\langle a \rangle$ does not agree with the results of Müller and Berlinger,[17] but in order to compare with the values given in that paper we must recognize that the term which they label a is 6 times larger than the parameter which we labeled a. However, even after dividing their values by 6 to compare with our results, their results are still a factor of 2–3 times larger than ours. Their pressure range, however, was so small that the discrepancy could be within their scatter, but their temperature range was much larger, and we do not know why their results differ so much from ours. Their values of a were measured in the cubic phase and showed a negative temperature dependence. Our values were measured in the tetragonal phase and give nearly zero-temperature dependence. They refer to the value

of a given by Hornig *et al.*[12] at room temperature in the tetragonal phase. This value agrees well with the result we would have at room temperature and atmospheric pressure but Müller and Berlinger's a versus temperature measurements do not extrapolate to that value.

Using Eqs. (8) we calculate $a=0.0461$ GHz, $b=0.0509$ GHz, and $\langle a\rangle=0.0493\pm0.0005$ GHz. Hornig *et al*. reported the value at room temperature of $12a+9b=0.95\pm0.21$ GHz. We get 1.011 ± 0.010 GHz, which is in very good agreement.

Müller and Berlinger used their large values of the temperature and pressure derivatives of a for $BaTiO_3$ as compared to those measured for other cubic oxides to argue for an enhanced anharmonicity of the Ti ion in $BaTiO_3$ and argue that it ''confirms the substantial order-disorder character in $BaTiO_3$.'' Our results negate those conclusions. We also conclude that there is a tricritical point in $BaTiO_3$ which is near $-33\,^\circ$C and 37 kbar.

ACKNOWLEDGMENTS

We are grateful to J. D. Barnett for helping us use his high-pressure EPR apparatus and many discussions of the work. We thank W. E. Evenson and D. H. Hatch for valuable critiques of the paper.

*Present address: Fairchild Semiconductor, West Jordan, UT 84088.

[1] G.A. Samara, Ferroelectrics **2**, 277 (1971).
[2] R.B. Griffith, Phys. Rev. Lett. **24**, 715 (1970)
[3] K. A. Müller, in *Structural Phase Transitions and Soft Modes*, edited by E. J. Samuelsen, E. Andersen, and J. Feder (University of Forlaget, Oslo, 1971), p. 85.
[4] W. Cochran, Adv. Phys. **9**, 387 (1960).
[5] R.B. Griffith, Phys. Rev. B **7**, 545 (1973).
[6] H.T. Evans, Jr., Acta Crystallogr. **14**, 1019 (1961).
[7] I.N. Polandov, B.A. Strukov, and V.P. Mylov, Sov. Phys. Solid State **9**, 1153 (1967).
[8] R. Clark and L. Benguigui, J. Phys. C **10**, 1963 (1977).
[9] D.L. Decker and Y.X. Zhao, Phys. Rev. B **39**, 2432 (1989).
[10] K. A. Müller and Th. vonWaldkirch, in *Local Properties at Phase Transistions*, Proceedings of the Enrico Fermi International School of Physics, Course LIX, Varenna, 1973, edited by K. A. Müller and A. Rigamonti (North-Holland, Amsterdam, 1976), Chap. II.
[11] K. A. Müller and J. C. Fayet, in *Structural Phase Transition II*, edited by K. A. Müller and H. Thomas (Springer-Verlag, Berlin, 1991), p. 1.
[12] A.W. Hornig, R.C. Rempel, and H.E. Weaver, J. Phys. Chem. Solids **10**, 1 (1959).
[13] E. Siegel and K.A. Müller, Phys. Rev. B **20**, 3587 (1979).
[14] K. A. Müller, in *Structural Phase Transitions and Soft Modes*, edited by E. J. Samuelsen, E. Andersen, and J. Feder (University of Forlaget, Oslo, 1971), p. 61.
[15] L. Rimai and A. deMars, Phys. Rev. **127**, 702 (1962).
[16] T. Sakudo, J. Phys. Soc. Jpn. **18**, 1626 (1962); T. Sakudo and H. Unoki, *ibid.* **19**, 2109 (1964).
[17] K.A. Müller and W. Berlinger, Phys. Rev. B **34**, 6130 (1986).
[18] M. H. Ellwanger, MS thesis, Brigham Young University, Provo, UT, 1984.
[19] J.D. Barnett, D.L. Decker, and M.H. Ellwanger in *High Pressure in Science and Technology*, edited by C. Homan, R. K. MacCrone, and E. Whalley, MRS Symposia Proceedings No. 22 (Materials Research Society, Pittsburgh, 1984), Pt. I, p. 184.
[20] Ke Huang, Ph.D. thesis, Brigham Young University, Provo, UT, 1995.
[21] Ke Huang, D.L. Decker, H.M. Nelson, and J.D. Barnett, Rev. Sci. Instrum. **68**, 3877 (1997).
[22] G.J. Piermarini, S. Block, J.D. Barnett, and R.A. Forman, J. Appl. Phys. **46**, 2774 (1975).
[23] K.A. Müller, W. Berlinger, and J. Albers, Phys. Rev. B **32**, 5837 (1985).
[24] E.J. Huibregtse and D.R. Young, Phys. Rev. **98**, 1562 (1956).
[25] J. Íñiguez, S. Ivantchev, J.M. Perez-Mato, and A. García, Phys. Rev. B **63**, 144103 (2001).